

www.acsami.org Research Article

# Heteroacene-Based Polymer with Fast-Switching Visible—Near Infrared Electrochromic Behavior

Tharindu A. Ranathunge, Christine Curiac, Kevin A. Green, Wojciech Kolodziejczyk, Glake Hill, Sarah Morgan, Jared H. Delcamp, and Davita L. Watkins\*



Cite This: ACS Appl. Mater. Interfaces 2023, 15, 7217–7226



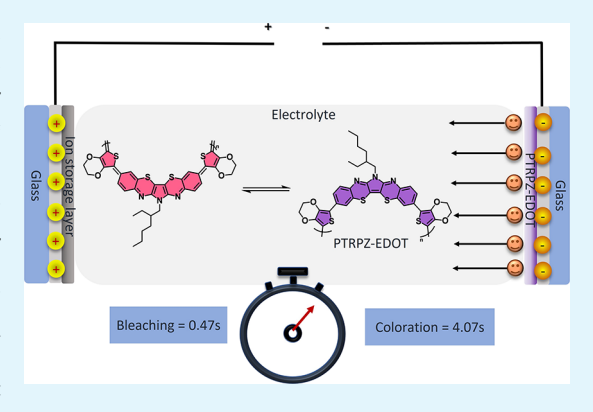
**ACCESS** I

III Metrics & More

Article Recommendations

s Supporting Information

ABSTRACT: The electrochromic properties and application of electronically conducting polymers (ECPs) (PTRPZ-EDOT) consisting of a 3,4-ethylenedioxythiophene (EDOT) and the heteroacene-based molecular scaffold, 6H-pyrrolo[3,2-b:4,5-b'] bis [1,4] benzothiazine (TRPZ), are reported. Known for its high electron mobility and conducting properties, the novel TRPZ scaffold was synthesized to possess two EDOT molecules termini affording TRPZ-EDOT. Electropolymerization of TRPZ-EDOT resulted in remarkable spectroscopic and conductive properties suitable for electrochromic device fabrication. Using atomic force microscopy (AFM), the average surface roughness and surface topography of PTRPZ-EDOT polymer thin films were determined. Spectroelectrochemical data showed that the polymer achieved switching times of 4.07 (coloration) and 0.47 s (bleaching) at 539 nm. The PTRPZ-EDOT film exhibits an optical contrast of 36–44% at 539 nm between its neutral and colored states, respectively.



The NIR region from 1000 to 1700 nm shows the appearance of charge carrier bands with a 0-1 V potential range. An electrochromic device was successfully fabricated from **PTRPZ-EDOT**, showcasing the potential and applicability of the polymer material for advanced technologies such as smart windows, flexible electrochromic screens, and energy storage devices.

KEYWORDS: electropolymerization, electrochromism, spectroelectrochemistry, heteroacene, semiconductors

# **■ INTRODUCTION**

Electrochromism is the color transition of a material in response to an applied electric field. Today, electrochromic materials have achieved application in electrochromic transistors, energy-saving tinted windows, infrared camouflage in the military, color displays, paper-based sensors, energy-storing devices, and supercapacitors. Optical properties are reversible in electrochromic materials when the material is oxidized or reduced electrochemically. Numerous inorganic and organic materials are reported as abundant and attractive electrochromic materials. The library of materials includes inorganic metal oxides, organic-small molecules, metal—organic frameworks, and polymeric materials.

Despite their abundance, durability issues like electrochemical degradation and morphology instability are factors that could be improved to promote large-scale fabrication. Additionally, switching times and optical contrast are essential factors for electrochromic devices since many applications require a clear to colored state transition. Although some electrochromic materials have multiple color states, a significant concern is the lack of complete transition into a colorless state. <sup>15</sup> Among the electrochromic materials showing transparent to colored states, organic small molecular viologens and their derivatives are common. However, slow switching

times and safety hazards of such liquid-state devices are of major concern. <sup>16</sup> Dopants such as multiwalled carbon nanotubes (MWCNTs) have been shown to improve kinetic switching, but the prolonged stability is questionable due to chemical degradation. <sup>17</sup>

Among polymeric materials, conventional electrochromic devices often employ polyaniline (PANI) or poly(3,4-ethylenedioxythiophene) (PEDOT). PANI is a good benchmark material for infrared (IR) active electrochromism and device fabrication. More commonly, EDOT-based polymers have been used as the primary electrochromic material due to their stability, oxidative state conductive properties, and coloration efficiency. PEDOT films are typically synthesized and fabricated using electrostatic deposition, However, challenges in applicability typically surround the low solubility of the polymer in fabricating solvents, thus hindering thin film

Received: November 23, 2022 Accepted: January 9, 2023 Published: January 24, 2023





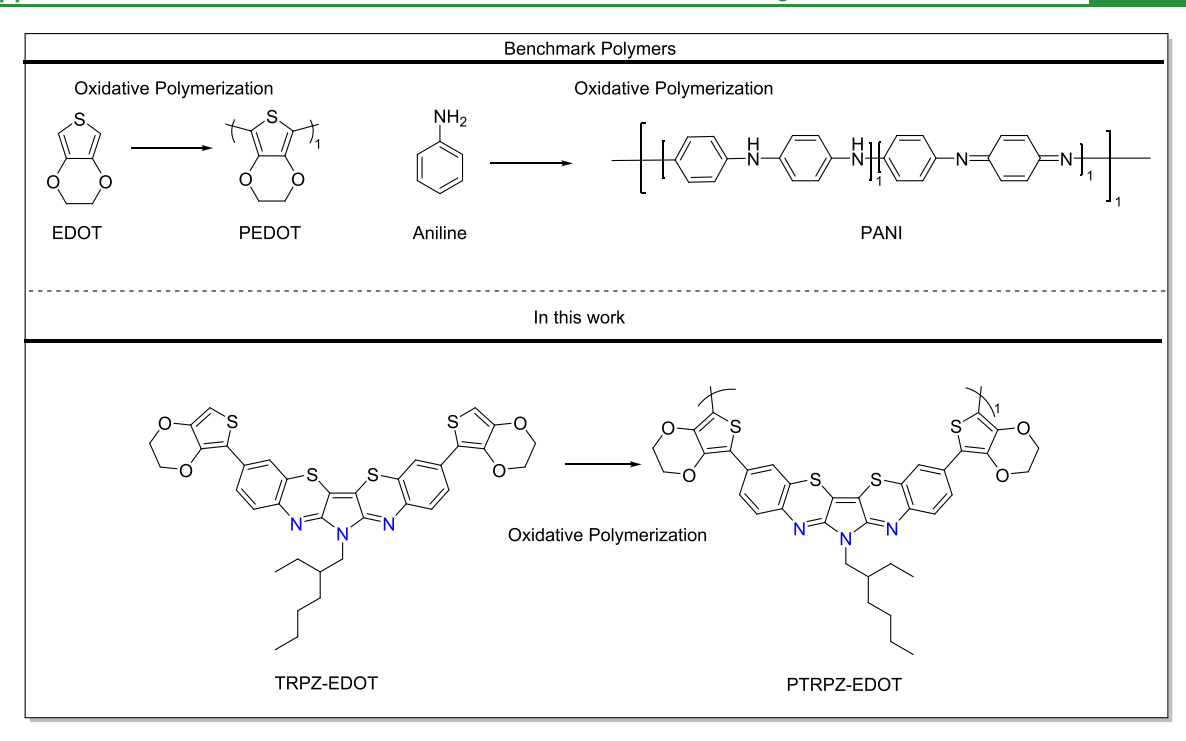


Figure 1. Oxidatively polymerized electrochromic materials.

preparation and overall device performance.<sup>24</sup> Poly(3,4-ethylenedioxythiophene):Poly(styrene sulfonate) or PEDOT:PSS is commonly used as an alternative that reduces the burdens associated with PEDOT.<sup>25</sup> Additionally, PEDOT:PSS has shown value as an ion storage domain and stabilizing layer for many optoelectronic devices.<sup>26</sup> Several studies have shown that electropolymerization conditions (i.e., solvents, thermoelectric, and electrolytes) for PEDOT can affect overall material properties.<sup>27–29</sup> Recently, the morphological and electrochromic properties of PEDOT derivative films were shown to possess a high contrast ratio, transparency in the doped state, and a high coloration efficiency due to improved strategic molecular designs.<sup>30</sup>

In this work, we present the molecular engineering of an EDOT-functionalized heteroacene (6H-pyrrolo[3,2-b,4,5-b'] bis [1,4] benzothiazine; TRPZ), which is then electropolymerized to give PTRPZ-EDOT, a conjugated polymer exhibiting both conductive and electrochromic behavior. The performance of PTRPZ-EDOT was compared to benchmark polymers, PEDOT and PANI. The structures of interest are shown in Figure 1.

TRPZ is a conjugated heteroacene  $\pi$ -system used in the fabrication of organic-field effect transistor (OFET) devices for p-type semiconductors. These devices have shown performances with average hole electron mobilities as high as  $0.34~\rm cm^2~\rm V^{-1}~\rm S^{-1}$  and an on/off ratio of about  $10^6-10^{7.31}$  To convert TRPZ into an electrochromic material, the TRPZ scaffold is flanked by two EDOT groups. We hypothesize that the TRPZ-scaffold will facilitate higher mobility of holes when between two EDOT groups and be stabilized in the oxidized state. We speculate that the faster hole transfer rate results in a faster switching time of the electrochromic material.  $^{31,32}$  Additionally, TRPZ is reported to show proaromaticity confirmed by computational calculations, which we believe can be used to maintain a stable oxidized state and prevent chemical degradation.  $^{33}$ 

An ethyl hexyl group is placed on the core nitrogen atom of TRPZ for solubility. The terminal ends of the TRPZ core were coupled to the EDOT molecule through direct arylation to synthesize the monomer unit, TRPZ-EDOT. Then, the monomer was electropolymerized to obtain PTRPZ-EDOT thin films. The electrochemical behaviors, surface morphologies, and electrochromic properties of the polymer were investigated systematically. In addition, an electrochromic device was fabricated using PTRPZ-EDOT as the electrochromic layer and platinum-plated fluorine-doped tin oxide (FTO) as an ion storage layer.

#### **EXPERIMENTAL METHODS**

**Materials.** All the chemical reagents and solvents involved in the experiment were purchased from Sigma-Aldrich and used without further purification unless otherwise specified. All molecular synthetic procedures were carried out under an inert-nitrogen or argon atmosphere using standard Schlenk line techniques. The electronic Supporting Information (SI) gives additional information regarding synthetic details, characterization, and general procedures.

Characterization. Nuclear magnetic resonance (NMR): <sup>1</sup>H and <sup>13</sup>C spectra were recorded on a Bruker Avance 400 MHz spectrometer with tetramethyl silane (TMS) as the internal standard. Mass spectra were collected via high-resolution mass spectrometry (HRMS), and quadruple-TOF was used to obtain the data both in positive and negative modes. Fourier-transform infrared (FT-IR) spectra were measured using a Bruker Alpha Fourier-transform infrared spectrophotometer.

Cyclic voltammogram (CV) curves were measured with a CH Instruments electrochemical analyzer (CHI-600E or CHI-602E). Solution measurements were taken using a platinum counter electrode, a saturated calomel reference electrode (SCE), and a glassy carbon working electrode. Film measurements were taken using a platinum counter electrode, SCE reference, and working electrode comprising a polymer deposited on fluorine-doped tin oxide (FTO)-coated glass slide. The electrolyte was 0.1 M tetrabutylammonium hexafluorophosphate (Bu<sub>4</sub>NPF<sub>6</sub>) in dichloromethane (DCM) for solution and film measurements. Ferrocene was used as a standard to calibrate the reference electrode with glassy carbon for the solution

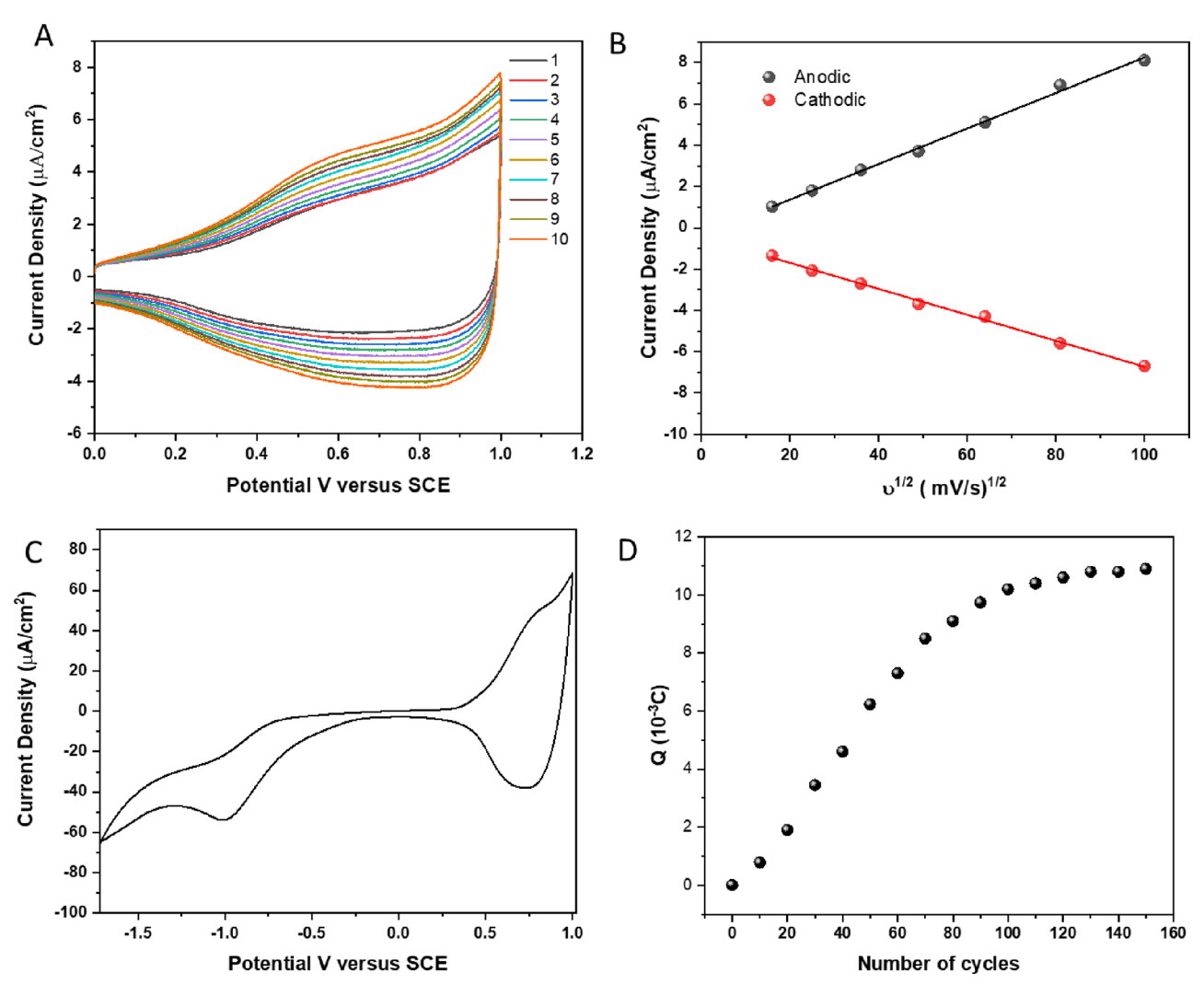


Figure 2. (A) CVs representing electropolymerization of TRPZ-EDOT in  $CH_2Cl_2-Bu_4NPF_6$  (0.1 M) solution (anodic and cathodic currents are show in a gradient for cycles 1 to 10). (B) Dependence of anodic and cathodic currents on the scan rates of 10 to 100 mV/s measured in the  $CH_2Cl_2-Bu_4NPF_6$  (0.1 M) system. (C) **PTRPZ-EDOT** CV recorded in a monomer-free solution of  $Bu_4NPF_6$  (0.1 M). (D) Changes in charge integrated over the cyclic voltammograms as a function of deposition cycles.

measurements. All potentials are with respect to the SCE unless otherwise stated. In each experiment, the solution was degassed by purging with high purity argon gas for 10 min, and a steady flow of argon gas was maintained above the solution to prevent re-entry of air. Electropolymerization was performed via 10 repetitive CVs by selecting a potential range between 0.0 and +1.0 V to prevent overoxidation. The polymer films obtained on the working electrode surface were cleaned with acetone to remove small organic residues, and the film was dried in a vacuum oven at 50 °C before obtaining ultraviolet-visible-near infrared-short wavelength infrared (UVvis-NIR-SWIR) spectra. The optical absorbance (UV-vis-NIR) spectra were measured with a Cary 5000 spectrophotometer on the samples deposited on the FTO substrate. The CV and AC impedance characteristics were recorded in an argon-purged neat background electrolyte (BGE) without monomers. CVs were recorded in the potential range within -1.0 to +1.0 V to oxidation and reduction peaks of the polymers in this range with a scan rate of 100 mV s<sup>-1</sup> unless otherwise indicated. Nyquist and Bode plots of AC impedance characteristics were reported in the frequency range of  $0.1\ Hz$  to 1MHz at applied potential bias values from -1 to +1 V range.

Spectroelectrochemistry data were collected with a modified spectroelectrochemical cell system (Pine Research Instrumentation) using a 1 cm × 1 cm quartz cuvette (Pine Research part RRPG094), platinum wire counter electrode, SCE reference, and polymer deposited FTO glass (shown in Figure S8). The electrodes are

connected to a potentiostat using crocodile clips (CH Instruments electrochemical analyzer, CHI600E), an Avantes/AvaSpecULS2048-USB2-50 spectrometer (Pine Research part RRAVSP3) with Avantes/AvaSpec light source (Pine Research part RRAVSP) and AvaSoft8 software program, Ocean Insight Flame-NIR+ spectrometer (FLMN02855) with Ocean Insight Halogen light source (HL-2000), and Ocean Insight OceanView software program to produce the absorption spectra and transmittance spectra. Simultaneously, the electrochemical data was acquired using CHI software. The surface topography was characterized using atomic force microscopy (AFM) in peak-force tapping mode (Bruker Dimension Icon) RTESPA-300 Tip.

Synthesis of PTRPZ-EDOT Thin Film. The single-step electropolymerization method was implemented with monomers, as previously reported. In brief, the TRPZ-EDOT monomer was dissolved in 10.0 mL to give a  $1\times 10^{-3}$  M solution of monomer. Calculated amounts are presented in Table S1. To the solution, tetrabutylammonium hexafluorophosphate (TBAHP; Bu<sub>4</sub>NPF<sub>6</sub>) BGE (0.1 M in DCM) was added. PEDOT and PANI thin films were synthesized according to methods adapted from the literature. <sup>18,35–37</sup>

Fabrication of Electrochromic Device. The electrolyte layer polymethylmethacrylate/polycarbonate/acetonitrile/tetrabutylammonium hexafluorophosphate (Bu<sub>4</sub>NPF<sub>6</sub>/PMMA/PC/MeCN: weight ratio of 3:7:20:70) and the Pt counter electrode were prepared in advance. As adopted from previous research,<sup>38</sup> PMMA was first

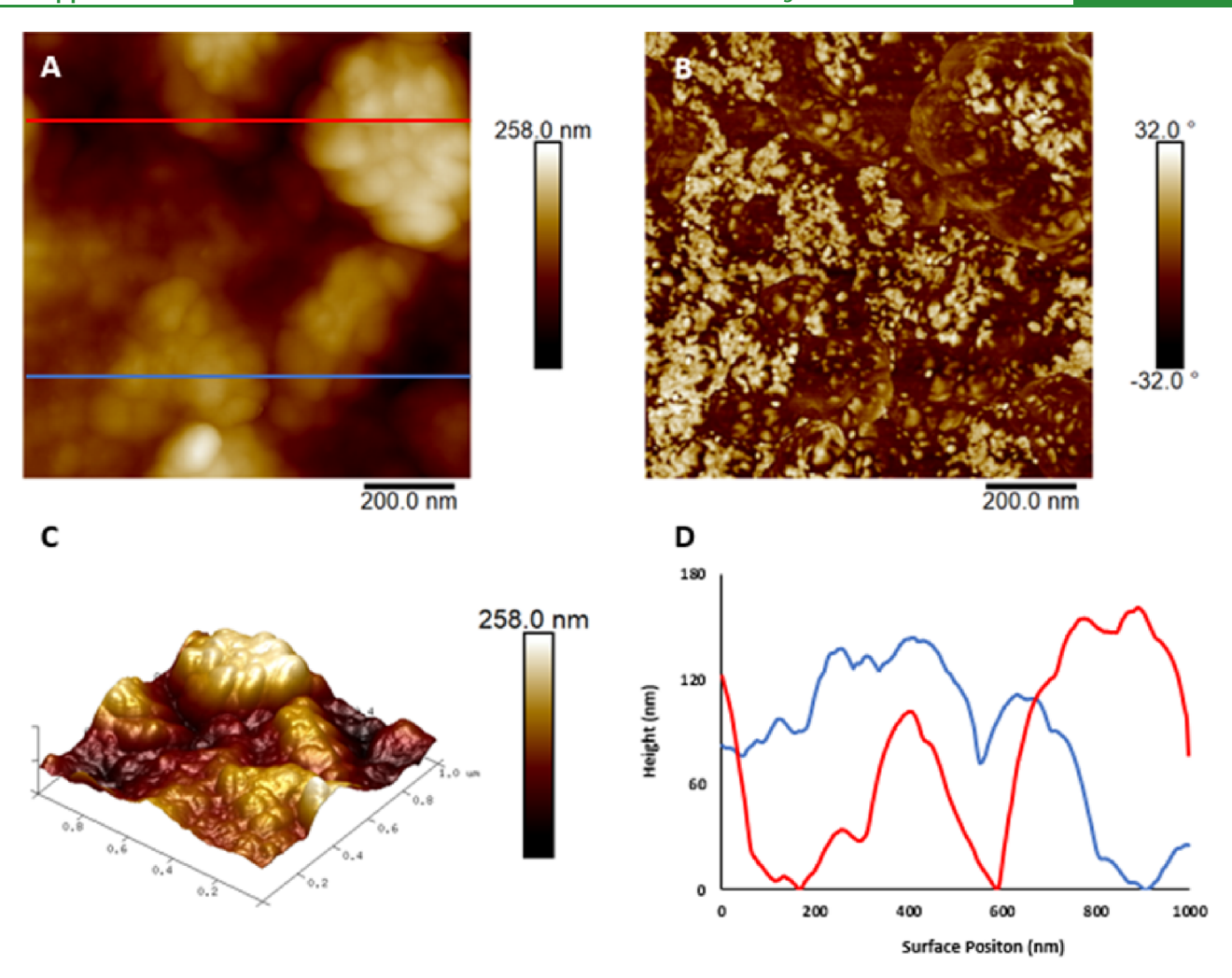


Figure 3. AFM images of PTRPZ-EDOT thin films on FTO glass substrate using peak force tapping mode. (A) Topographic (height), (B) phase, (C) 3D topographic, and (D) cross-sectional topographic.

dissolved in PC solution (0.1 M) at 80 °C, and then a 0.1 M solution of  $Bu_4NPF_6$  in MeCN was added. Finally, the volatiles (70% MeCN) were evaporated to give a sol–gel electrolyte. Device fabrication and Pt electrodes follow the previously reported literature. <sup>39,40</sup> In brief, the Pt electrodes were prepared using TEC 7 FTO-coated glass (Hartford Glass Co), and the polymer film electrodes were prepared using TEC 10 FTO-coated glass (Hartford Glass Co) and were cleaned and prepped for device fabrication, as previously mentioned and reported above. Solid-state devices were fabricated and sealed with the polymer film on TEC 10 glass as the electrochromic layer, PMMA/PC/MeCN/Bu<sub>4</sub>NPF<sub>6</sub> as the electrolyte layer, and Pt on TEC 7 glass as the ion storage layer.

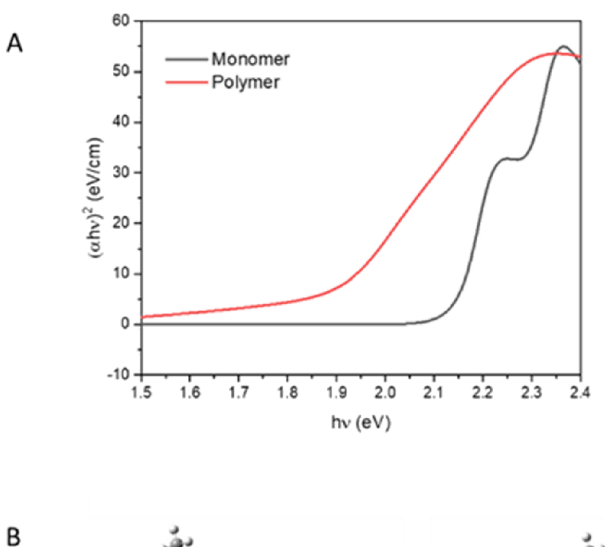
#### RESULTS AND DISCUSSION

**Electropolymerization.** The electropolymerization of the monomer TRPZ-EDOT was carried out in the  $CH_2Cl_2$ –  $Bu_4NPF_6$  (0.1 M) electrolyte system. The electrochemical properties of the monomer were analyzed using a monomer in  $Bu_4NPF_6$  (0.1 M) with CV obtained from -1 to +1 V potential range (shown in Figure S9). The CV shows a redox couple in the anodic direction of the x-axis starting from 0.4 to 1.2 V. Figure 2A shows 10 repetitive CVs for the polymerization at a 1.0 V switching potential. The rate of polymerization was determined by the current density comparison between the first scan, 0.694 V ( $j = 2.61 \ \mu A/cm^{-2}$ ), and the last scan, 0.670

V ( $j = 4.15 \ \mu\text{A/cm}^{-2}$ ), which is 1.59 times higher than the initial scan.

After 10 repetitive CVs, a thin film of the homopolymer PTRPZ-EDOT is deposited on the surface of the glassy carbon working electrode. The plot of scan rate (v) against the maximum current density of the anodic wave at 0.58 V and the cathodic wave at 0.81 V shows a linear relationship (Figure 2B). However, the accuracy of the curves decreases with lower scan rates as seen via a large positive intercept as  $v^{1/2}$  approaches zero at about 2.5–3.0  $\mu$ A cm<sup>-2</sup>.

Figure 2C shows the CV of the PTRPZ-EDOT polymer deposited after 10 repetitive cycles onto the glassy carbon electrode and then introduced to a monomer free 0.1 M  $\rm CH_2Cl_2-Bu_4NPF_6$  solution. A redox couple was observed in a sweep from 0 to 1 V (Ep), where the anodic shoulder current density is detected at 0.77 V ( $j=47~\mu A/\rm cm^{-2}$ ) and the cathodic peak is detected at 0.70 V ( $j=-38~\mu A/\rm cm^{-2}$ ). The return sweep from 0 to  $-1~\rm V$  shows a redox couple of the anodic peak at  $-0.77~\rm V$  ( $j=-7~\mu A/\rm cm^{-2}$ ) as a shoulder and a cathodic peak at  $-1.04~\rm V$  ( $j=-54~\mu A/\rm cm^{-2}$ ). We conducted the experiments by changing the different number of deposition cycles and then determined the charge stored at the end of each deposition. Note that this does not denote the reaction rate yet describes the charge stored in the electropolymerized thin film. The charge steadily increased linearly



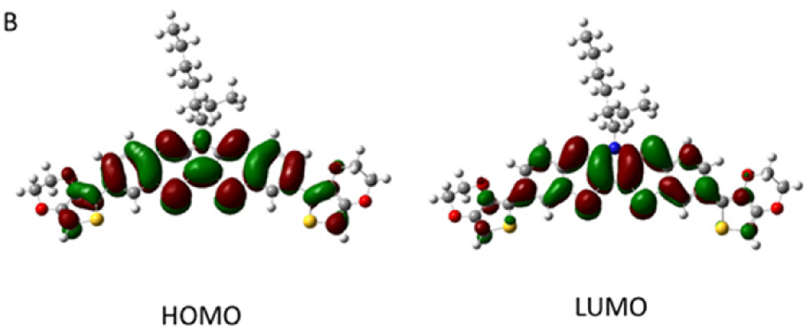


Figure 4. (A) Tauc plot of TRPZ-EDOT and PTRPZ-EDOT and (B) frontier molecular orbital pictures for TRPZ-EH-EDOT using the B3LYP/a 6-31 g (d, p) basis set method.

from the initial cycles up to 70 and began to plateau from 80 to 150 cycles (Figure 2D).

Electrochemical impedance spectroscopy (EIS) of the thin-film polymer was investigated within the potential range from -1 to 1 V. AC impedance analysis was used to assess the electrical properties of the film. Representative Nyquist plots of PTRPZ-EDOT and an equivalent circuit (Figures S10–S12) were used to draw a fitting data plot to analyze electrical parameters shown in Table S1. The electrical parameters were extracted by fitting the experimental plots to theoretical ones generated from the equivalent circuit. A dual-rail transmission-line circuit and a simplified equivalent circuit used for data extraction are also shown in Figure S10. Typical of many conducting polymers, PTRPZ-EDOT shows noticeable average electron transport resistance (Re) values in the ptype (i.e., positive or cationic domain, oxidation) regime in the range from 754 to 770  $\Omega$ .

In contrast, the n-type regime shows Re values from 698 to 738  $\Omega$ , with slightly lower resistance than in the positive domain. The electrical conductivity data corroborates well with the trend in the CV of the polymer in the BGE, where it shows high currents in the potential region between -1.0 and +1.0 V with higher values at the ends. Interestingly, the Warburg impedance (W) representing ion transport resistance by diffusion is much lower (10 to 40  $\mu\Omega$ ) in potential regimes where the polymer has higher Re values. In the p-type regime, W values are between 34.1 and 33.7  $\mu\Omega$ , while in the n-type regime, values are between 16.5 and 23.5  $\mu\Omega$ .

**Surface Morphology Characterization.** AFM images of **PTRPZ-EDOT** films formed at different deposition cycles were obtained in peak-force tapping mode, as described in the

Experimental Methods section. The topographic image of the film obtained from 20 deposition cycles (Figure 3A) displays an irregular surface with raised clusters of globular features and significant roughness (root mean square (RMS) roughness of 43 nm, maximum height (Rmax) of 258 nm). The phase image (Figure 3B) reveals similar features with brighter areas generally tracking with the topography observed in the height image. No clear phase separation or crystalline features are observed in the phase image. The surface roughness and irregularity are further evidenced in three-dimensional topographic and horizontal cross-sectional traces (Figure 3C,D), where local variations of greater than 100 nanometers are observed. AFM analysis of films produced with additional deposition cycles (40, 60, 80, 100, and 150 cycles) shows that surface roughness is not substantially reduced until 150 cycles are employed (Figure S13). The 150-deposition cycle film demonstrates an Rmax of 156 nm and an RMS of 23 nm. The smoother surface may enhance conductivity and facilitate large-scale device fabrication.<sup>38</sup>

Comparative surface topography studies were performed on conventional polymers, PEDOT and PANI. AFM analysis reveals elongated fibrillar structures, assumed to be crystallites, in both height and phase images for both systems. The crystallites are observed as bright raised features in topography and brighter (harder) surfaces in-phase images, with lengths of 100–200 nm and widths of 20–50 nm (Figures S14 and S15). Surfaces are rough for both PEDOT and PANI, with RMS values of 80.4 and 94.3 nm, respectively, in a range similar to that observed for PTRPZ-EDOT films.

**Photophysical Properties.** The UV-vis-NIR spectrum of the TRPZ-EDOT monomer is shown in the SI (Figure

S16). TRPZ-EDOT shows absorbance maximum centered at 525 nm. The optical band gap calculated by Tauc plot analysis of the monomer shows at 2.13 eV (Figure 4A and Table 1). The electrochemical energy gap was calculated using cyclic voltammetry, which shows a HOMO of -4.69 and LUMO of -2.09 eV, yielding a band gap of 2.60 eV.

Table 1. Photophysical Properties of the Monomer TRPZ-EDOT in THF and Thin-Film Polymer PTRPZ-EDOT in the Solid State

	$E_{\rm g}^{ m opt}({ m eV})$	$\lambda_{abs}^{max}$ (nm)	HUMO <sup>CV</sup> (eV)	LUMO <sup>CV</sup> (eV)	$E_{\rm g}^{\rm CV}({ m eV})$
TRPZ- EDOT	2.13	494	-4.69	-2.09	2.60
PTRPZ- EDOT	1.86	539	-5.14	-4.21	0.93

PTRPZ-EDOT thin-film absorbance spectra are shown in the SI (Figure S17). The solid-state polymer absorbance maximum is 539 nm in the visible range. A wide absorbance band was observed starting from 1100 to 1900 nm where it centered at 1604 nm, which corresponds to the polaron band

of the p-doped state of the polymer. The optical band gap of the solid-state polymer onset is 1.83 eV.

Supporting computational calculations show a peak absorbance maximum at 510 nm of the gaseous phase monomer using the B3LYP method with a 6-31 g (d, p) basis set. Frontier molecular orbitals and calculated absorbance spectra are shown in Figure 4B and Figure S18. The theoretical band gap of the monomer is 2.59 eV in THF. The gas phase DFT calculations show a higher band gap than that of the experimental optical band gap (Figure S18). Molecular orbitals of the monomer at HOMO energy show an electron distribution starting from EDOT to the pyrrole ring. LUMO energy shows the electron distribution only within the phenyl and pyrrole rings as it regains aromaticity.

Spectroelectrochemistry and Switching Behavior. Figure 5A shows UV-vis-NIR absorption spectra of a PTRPZ-EDOT thin film under different applied potentials (experimental setup shown in Figure S8). At 0 V applied potential, a well-defined absorption band centered at 539 nm is observed, which can be ascribed to the pi to pi\* electronic transition of the p-doped state polymer backbone. With increasing applied potential, the intensity of the 539 nm peak

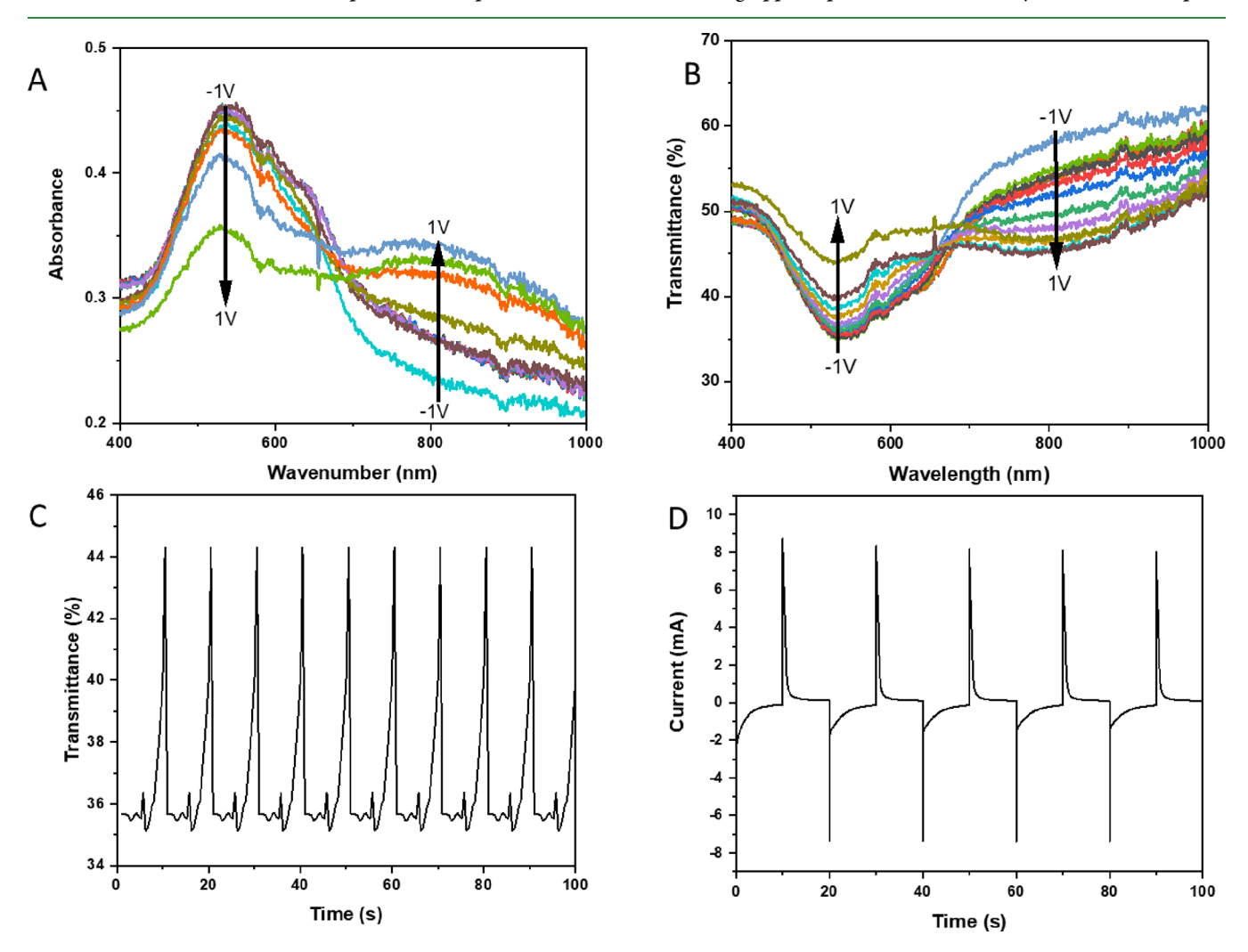


Figure 5. Spectroelectrochemical data of a PTRPZ-EDOT film on the FTO glass under different applied potentials in 0.1 M  $CH_2Cl_2-Bu_4NPF_6$  solution were collected as either absorption (A) or transmittance (T %) (B) versus wavelength (nm) (note that spectra are overlapping from -1 to 1 V potential). Optical contrasts of a PTRPZ-EDOT film monitored at 539 nm in 0.1 M  $CH_2Cl_2-Bu_4NPF_6$  solution between 0 and 1.0 V (C) and electrochemical kinetics (D).

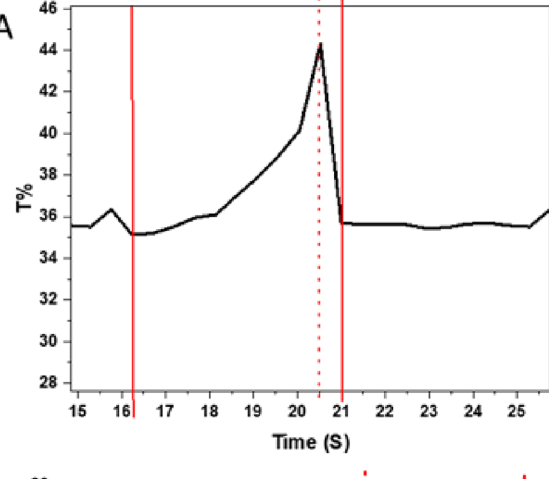
decreases, indicating that oxidation of monomer units and the doping of counterions in the polymer backbone alters the band gap of PTRPZ-EDOT. The attenuation in the main band at 539 nm is accompanied by the appearance of charge carrier bands at around 700 and 1000 nm that arise from the evolution of the bipolaron band. The peak centered at 539 nm molecular absorbance does not entirely transform to a different state in Figure 5A. The experiment was carried out in transmittance (%) mode, where a similar trend was observed, as shown in Figure 5B.

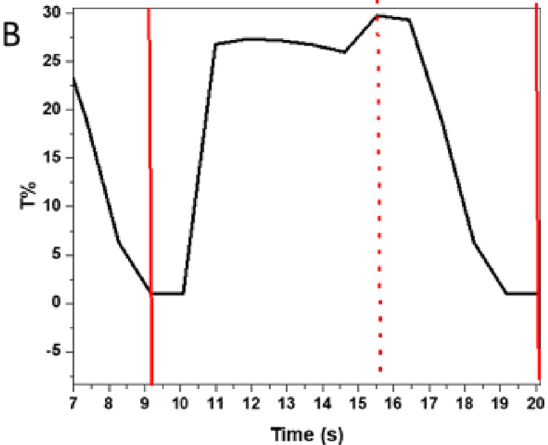
Figure 5C displays optical contrasts of the PTRPZ-EDOT film, which exhibits a 36 to 44% contrast at 539 nm between its neutral and oxidized states. Figure 6 exhibits the switching response of a PTRPZ-EDOT film at 539 nm. The electrochromic switching performance of the PTRPZ-EDOT film was examined with a residence time of 5 s at the visible range (539 nm) between 0 and 1.0 V. The color to bleach switching time is the time required to reach 90% of the total change in absorbance after switching the potential.<sup>41</sup> At 539 nm, the switching time is 4.07 s for coloring and 0.47 s for bleaching. The optical contrast and rapid switching time make the PTRPZ-EDOT film an excellent electrochromic material relative to other EDOT derivatives. 42 The current density versus time plot shows multiple switching steps for PTRPZ-EDOT film (Figure 5D). Chronoamperometry curves are useful for comparing the electrochromic behavior before and after device fabrication. The potential was applied for 10 s at -1.0 V for reduction and 10 s at +1.0 V for oxidation, which shows a quick response time of less than 1 s. The stability of the PTRPZ-EDOT film was investigated using transmittance at 539 nm over 10,000 cycles, which slightly decreased from 44.3 to 43.9% in Figure S19.

These results were compared with conventional electro-chromic polymer PEDOT and PANI. For PEDOT, the visible absorbance maximum is 550 nm (Figure S20A). In contrast, PANI showed an absorbance maximum at 435 nm (Figure S21A) and completely changed to the polaron band arising from 600 nm. The optical contrast of PEDOT is 10% contrast at 550 nm between different oxidation states (Figure S20B), while PANI has a 25% contrast at 613 nm (Figure S21B). However, the coloration times (8.59 s PEDOT and 6.04 s PANI) and bleaching times (2.85 s for PEDOT and 4.54 s for PANI) for PEDOT and PANI are comparatively longer than those for PTRPZ-EDOT (Figure 6B, C).

The near-IR (NIR) region from 1000 to 1700 nm shows the appearance of charge carrier bands with increasing applied potentials (Figure S22A-D). Unlike PEDOT, PTRPZ-EDOT has an absorbance maximum of 1604 nm. We hypothesized that the NIR range band corresponds to the bipolaron developed in the polymer backbone. PTRPZ-EDOT has a relatively higher optical contrast than PEDOT from the 1000 to 1700 nm region (Figure S22B,D). The PTRPZ-EDOT optical contrast at 1176, 1381, and 1620 nm in 0.1 M CH<sub>2</sub>Cl<sub>2</sub>-Bu<sub>4</sub>NPF<sub>6</sub> solution between 0 and 1.0 V with a residence time of 5 s was reported (Figure S23A). For PTRPZ-EDOT, 13 to 16.9% contrast at 1176 nm, 12 to 15.6% contrast at 1382 nm, and 6.6 to 9.9% contrast at 1620 nm were reported. Comparatively, PEDOT shows a lower optical contrast with 2.85% contrast at 1170 nm and 2.46% contrast at 1376 nm (Figure S23B).

Electrochromic Properties of Solid-State Electrochromic Device. Electrochromic devices based on PTRPZ-EDOT, PEDOT, and PANI were evaluated for practical





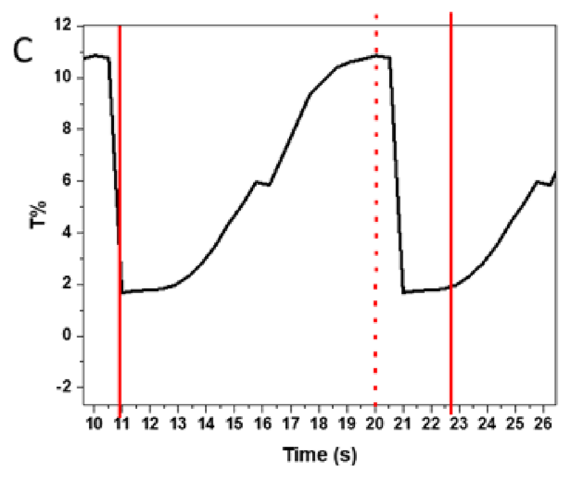


**Figure 6.** Switching response of (A) PTRPZ-EDOT film at 539 nm, (B) PANI film at 592 nm, and (C) PEDOT film at 550 nm.

applications by investigating their performance. Chronoamperometry was used to measure current consumption and the amount of charge transferred during each switch. The all-solid-state electrochromic devices (2.0 cm  $\times$  2.0 cm) consisting of polymer thin film were assembled as detailed in the fabrication of the electrochromic device section above. The devices show that increasing the applied potential leads to color switching from a neutral state (0 V) to a colorless state (1 V), as shown in Figure S24C,D, and Video S1, where the colorless state is conductive and the colored state is nonconductive.

Devices were also fabricated using benchmark polymers PANI and PEDOT (Figure S24A,B,E,F, Videos S2 and S3).

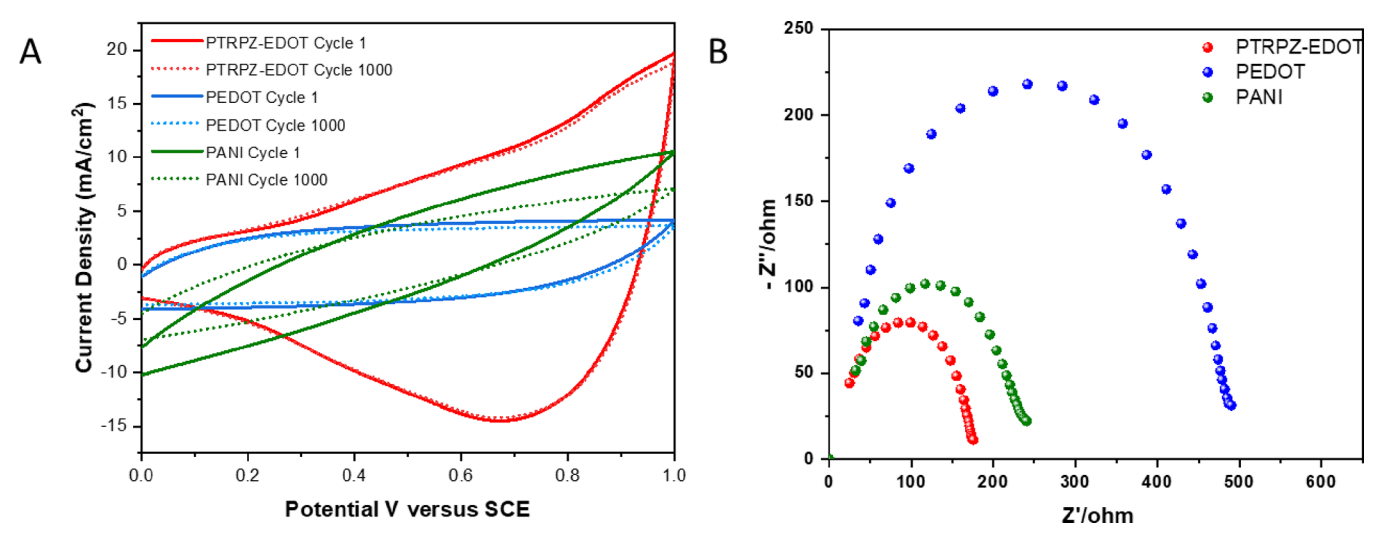


Figure 7. (A) Electrochemical stability and (B) Nyquist Plot PTRPZ-EDOT, PEDOT, and PANI devices.

The electrochemical stability of the devices was analyzed using cyclic voltammetry, which shows a deviation in the first oxidation peak current density over 1000 cycles (Figure 7A). The cyclic voltammogram shows that the PTRPZ-EDOT is stable over 1000 cycles. In comparison, the EDOT device shows no significant difference after 1000 cycles. However, the PANI device shows a significant change after 1000 cycles.

Electrochemical impedance spectroscopy (EIS) experiments were also conducted on the devices at an open-circuit potential bias to probe electron transfer resistances. EIS experiment shows the resistance of 174  $\Omega$ , corresponding to the resistance developed by the thin film on the electrode, for PTRPZ-EDOT. The resistance is drastically lower than the conventional polymers PANI (251  $\Omega$ ) and PEDOT (492  $\Omega$ ) (Figure 7B). Overall, PTRPZ-EDOT has promising electrochromic properties for the possibility of manufacturing at a large-scale with potential applications for pseudocapacitors, flexible electrochromic screens, sunglasses, and smart windows.

# CONCLUSIONS

PTRPZ-EDOT is a 3,4-ethylenedioxythiophene derivative that has been synthesized and characterized in this project. This is, to the best of our knowledge, the first time a heteroacene piconjugated structure exhibiting proaromacity has been applied to the development of electrochemically switching polymer thin films. The detailed results show that the colored neutral states and the colorless or clear oxidized states of PTRPZ-EDOT under an applied potential exhibit a switch "on"switch "off" mechanism. The electrochemical redox potential for PTRPZ-EDOT thin films displays unique redox behavior and has capacitances greater than conventional polymers. Additionally, PTRPZ-EDOT thin films possess optical contrast at 539 nm with a fast-switching time of 4.07 s for coloring and 0.47 s for bleaching. The electrochromic devices of PTRPZ-EDOT have a similar pattern with a neutral color state to an oxidized colorless state and robust cyclic stability over 1000 cycles. The electrochromic performance for PTRPZ-EDOT presents outstanding electrochromic behavior with a low transmittance percentile. Future studies will investigate device transmittance properties and further apply the materials to more advanced electrochromic devices.

#### I ASSOCIATED CONTENT

# Supporting Information

The Supporting Information is available free of charge at https://pubs.acs.org/doi/10.1021/acsami.2c21111.

Experimental procedures and characterization for all new compounds, <sup>1</sup>H and <sup>13</sup>C NMR spectral data, microscopy images, spectroscopic profiles, and electrochemical data (PDF)

Device operation and switching videos (ZIP)

# AUTHOR INFORMATION

## **Corresponding Author**

Davita L. Watkins — Department of Chemistry and Biochemistry, University of Mississippi University, Oxford, Mississippi 38677, United States; Department of Chemistry and Biochemistry, The Ohio State University, Columbus, Ohio 43210, United States; William G. Lowrie Department of Chemical and Biomolecular Engineering, The Ohio State University, Columbus, Ohio 43210, United States; orcid.org/0000-0002-0943-7220; Email: dwatkins@olemiss.edu, watkins.891@osu.edu

#### **Authors**

Tharindu A. Ranathunge — Department of Chemistry and Biochemistry, University of Mississippi University, Oxford, Mississippi 38677, United States; Department of Chemistry, Brown University, Providence, Rhode Island 02912, United States

Christine Curiac — Department of Chemistry and Biochemistry, University of Mississippi University, Oxford, Mississippi 38677, United States; ⊚ orcid.org/0000-0003-2468-8906

Kevin A. Green — School of Polymer Science and Engineering, University of Southern Mississippi, Hattiesburg, Mississippi 39406, United States; orcid.org/0000-0002-2539-3117

Wojciech Kolodziejczyk – Interdisciplinary Center for Nanotoxicity, Department of Chemistry, Physics and Atmospheric Sciences, Jackson- State University, Jackson, Mississippi 39217, United States; orcid.org/0000-0002-7754-8969

Glake Hill – Interdisciplinary Center for Nanotoxicity, Department of Chemistry, Physics and Atmospheric Sciences, Jackson- State University, Jackson, Mississippi 39217, United

Sarah Morgan - School of Polymer Science and Engineering, University of Southern Mississippi, Hattiesburg, Mississippi 39406, United States; o orcid.org/0000-0002-8796-9548

Jared H. Delcamp - Department of Chemistry and Biochemistry, University of Mississippi University, Oxford, Mississippi 38677, United States; o orcid.org/0000-0001-5313-4078

Complete contact information is available at: https://pubs.acs.org/10.1021/acsami.2c21111

#### **Author Contributions**

The manuscript was written through the contributions of all authors. All authors have approved the final version of the manuscript.

#### **Notes**

The authors declare no competing financial interest.

#### ACKNOWLEDGMENTS

The authors would like to thank the National Science Foundation (OIA 1757220) for providing the funding for this study.

## REFERENCES

- (1) Cao, X.; Lau, C.; Liu, Y.; Wu, F.; Gui, H.; Liu, Q.; Ma, Y.; Wan, H.; Amer, M. R.; Zhou, C. Fully Screen-Printed, Large-Area, and Flexible Active-Matrix Electrochromic Displays Using Carbon Nanotube Thin-Film Transistors. ACS Nano 2016, 10, 9816-9822.
- (2) Thambidurai, M.; Omer, M. I.; Shini, F.; Dewi, H. A.; Jamaludin, N. F.; Koh, T. M.; Tang, X.; Mathews, N.; Dang, C. Enhanced Thermal Stability of Planar Perovskite Solar Cells Through Triphenylphosphine Interface Passivation. ChemSusChem 2022, 15, No. e202102189.
- (3) Granqvist, C. G. Electrochromic Materials: Out of A Niche. Nat. Mater. 2006, 5, 89-90.
- (4) Gratzel, M. Ultrafast Color Displays. Nature 2001, 409, 575-576.
- (5) Liu, H.; Crooks, R. M. Paper-Based Electrochemical Sensing Platform with Integral Battery And Electrochromic Read-Out. Anal. Chem. 2012, 84, 2528-2532.
- (6) Wang, J.; Zhang, L.; Yu, L.; Jiao, Z.; Xie, H.; Lou, X. W.; Sun, X. W. A Bi-Functional Device for Self-Powered Electrochromic Window and Self-Rechargeable Transparent Battery Applications. Nat. Commun. 2014, 5, 4921.
- (7) Wei, D.; Scherer, M. R.; Bower, C.; Andrew, P.; Ryhanen, T.; Steiner, U. A Nanostructured Electrochromic Supercapacitor. Nano Lett. 2012, 12, 1857-1862.
- (8) Bessinger, D.; Muggli, K.; Beetz, M.; Auras, F.; Bein, T. Fast-Switching Vis-IR Electrochromic Covalent Organic Frameworks. J. Am. Chem. Soc. 2021, 143, 7351-7357.
- (9) Elool Dov, N.; Shankar, S.; Cohen, D.; Bendikov, T.; Rechav, K.; Shimon, L. J. W.; Lahav, M.; van der Boom, M. E. Electrochromic Metallo-Organic Nanoscale Films: Fabrication, Color Range, and Devices. J. Am. Chem. Soc. 2017, 139, 11471-11481.
- (10) Gillaspie, D. T.; Tenent, R. C.; Dillon, A. C. Metal-Oxide Films for Electrochromic Applications: Present Technology and Future Directions. J. Mater. Chem. 2010, 20, 9585-9592.
- (11) Hou, Y.; Kong, L.; Ju, X.; Liu, X.; Zhao, J.; Niu, Q. Multichromic Polymers Containing Alternating Bi(3-Methoxythiophene) and Triphenylamine Based Units with Para-Protective Substituents. Materials 2016, 9, 779.
- (12) Koo, B. R.; Ahn, H. J. Fast-Switching Electrochromic Properties of Mesoporous WO3 Films With Oxygen Vacancy Defects. Nanoscale **2017**, 9, 17788–17793.

- (13) Ming, S.; Zhen, S.; Lin, K.; Zhao, L.; Xu, J.; Lu, B. Thiadiazolo[3,4-c] pyridine as an Acceptor toward Fast-Switching Green Donor-Acceptor-Type Electrochromic Polymer with Low Bandgap. ACS Appl. Mater. Interfaces 2015, 7, 11089-11098.
- (14) Shah, K. W.; Wang, S. X.; Soo, D. X. Y.; Xu, J. Viologen-Based Electrochromic Materials: From Small Molecules, Polymers and Composites to Their Applications. Polymer 2019, 11, 1839.
- (15) Zhang, Y.; Zhang, Y.; Du, H.; Dong, Y.; Zhao, J.; Xie, Y. Electrochromic Behaviors of Novel Conjugated Copolymers Based on [1,2,5] Thiadiazolo[3,4-G] Quinoxaline, Carbazole and Cyclopentadithiophene Units: Multicolor Double-Doping and Low Band Gap. Org. Electron. 2022, 105, No. 106514.
- (16) Wu, J. T.; Liou, G. S. A Novel Panchromatic Shutter Based on an Ambipolar Electrochromic System Without Supporting Electrolyte. Chem. Commun. 2018, 54, 2619-2622.
- (17) Frolov, D. G.; Khorova, A. I.; Kharitonova, E. P.; Keshtov, M. L.; Makhaeva, E. E. Electrochromic Behavior of Poly(amine-amide) with Pendant N-Phenylcarbazole and Triphenylamine Units and Its Composite With Multiwalled Carbon Nanotubes. Mater. Today Commun. 2020, 25, No. 101369.
- (18) Korent, A.; Žagar Soderžnik, K.; Šturm, S.; Žužek Rožman, K. A Correlative Study of Polyaniline Electropolymerization and its Electrochromic Behavior. J. Electrochem. Soc. 2020, 167, 106504.
- (19) Zhang, L.; Wang, B.; Li, X.; Xu, G.; Dou, S.; Zhang, X.; Chen, X.; Zhao, J.; Zhang, K.; Li, Y. Further Understanding of The Mechanisms Of Electrochromic Devices With Variable Infrared Emissivity Based on Polyaniline Conducting Polymers. J. Mater. Chem. C 2019, 7, 9878-9891.
- (20) Groenendaal; Zotti; Aubert; Waybright; Reynolds, J. R. Electrochemistry of Poly(3,4-alkylenedioxythiophene) Derivatives. Adv. Mater. 2003, 15, 855-879.
- (21) Osterholm, A. M.; Ponder, J. F., Jr.; Kerszulis, J. A.; Reynolds, J. R. Solution Processed PEDOT Analogues in Electrochemical Supercapacitors. ACS Appl. Mater. Interfaces 2016, 8, 13492-13498.
- (22) Tseng, C. H.; Lin, H. H.; Hung, C. W.; Cheng, I. C.; Luo, S. C.; Cheng, I. C.; Chen, J. Z. Electropolymerized Poly(3,4-ethylenedioxythiophene)/Screen-Printed Reduced Graphene Oxide-Chitosan Bilayer Electrodes for Flexible Supercapacitors. ACS Omega 2021, 6, 16455-16464.
- (23) Zhang, S.; Ren, J.; Zhang, Y.; Peng, H.; Chen, S.; Yang, F.; Cao, Y. PEDOT Hollow Nanospheres for Integrated Bifunctional Electrochromic Supercapacitors. Org. Electron. 2020, 77, No. 105497.
- (24) Yano, H.; Kudo, K.; Marumo, K.; Okuzaki, H. Fully Soluble Self-Doped Poly(3,4-Ethylenedioxythiophene) with an Electrical Conductivity Greater Than 1000 S cm-1. Sci. Adv. 2019, 5, 2375-
- (25) Palumbiny, C. M.; Heller, C.; Schaffer, C. J.; Körstgens, V.; Santoro, G.; Roth, S. V.; Müller-Buschbaum, P. Molecular Reorientation and Structural Changes in Cosolvent-Treated Highly Conductive PEDOT: PSS Electrodes for Flexible Indium Tin Oxide-Free Organic Electronics. J. Phys. Chem. C 2014, 118, 13598-13606.
- (26) Kim, Y. H.; Sachse, C.; Machala, M. L.; May, C.; Müller-Meskamp, L.; Leo, K. Highly Conductive PEDOT: PSS Electrode with Optimized Solvent and Thermal Post-Treatment for ITO-Free Organic Solar Cells. Adv. Funct. Mater. 2011, 21, 1076-1081.
- (27) Poverenov, E.; Li, M.; Bitler, A.; Bendikov, M. Major Effect of Electropolymerization Solvent on Morphology and Electrochromic Properties of PEDOT Films. Chem. Mater. 2010, 22, 4019-4025.
- (28) Seki, Y.; Takahashi, M.; Takashiri, M. Effects of Different Electrolytes and Film Thicknesses on Structural and Thermoelectric Properties of Electropolymerized Poly(3,4-Ethylenedioxythiophene) Films. RSC Adv. 2019, 9, 15957-15965.
- (29) Saxena, N.; Keilhofer, J.; Maurya, A. K.; Fortunato, G.; Overbeck, J.; Müller-Buschbaum, P. Facile Optimization of Thermoelectric Properties in PEDOT: PSS Thin Films through Acido-Base and Redox Dedoping Using Readily Available Salts. ACS Appl. Energy Mater. 2018, 1, 336-342.
- (30) Kousseff, C. J.; Taifakou, F. E.; Neal, W. G.; Palma, M.; Nielsen, C. B. Controlling Morphology, Adhesion, and Electro-

chromic Behavior of PEDOT Films Through Molecular Design and Processing. J. Polym. Sci. 2021, 60, 504-516.

- (31) Hong, W.; Wei, Z.; Xi, H.; Xu, W.; Hu, W.; Wang, Q.; Zhu, D. 6H-Pyrrolo[3,2-b,4,5-b'] bis [1,4] benzothiazines: Facilely Synthesized Semiconductors for Organic Field-Effect Transistors. J. Mater. Chem. 2008, 18, 4814-4820.
- (32) Hong, W.; Wei, Z.; Xu, W.; Wang, Q.; Zhu, D. Synthesis and Properties of Heteroacenes Containing Pyrrole and Thiazine Rings as Promising n-Type Organic Semiconductor Candidates. Chin. J. Chem. 2009, 27, 846-849.
- (33) Ranathunge, T. A.; Yaddehige, M. L.; Varma, J. H.; Smith, C.; Nguyen, J.; Owolabi, I.; Kolodziejczyk, W.; Hammer, N. I.; Hill, G.; Flynt, A.; Watkins, D. L. Heteroacene-Based Amphiphile as a Molecular Scaffold for Bioimaging Probes. Front Chem. 2021, 9, No. 729125.
- (34) Ranathunge, T. A.; Karunathilaka, D.; Ngo, D. T.; Attanayake, N. H.; Brodgon, P.; Delcamp, J. H.; Rajapakse, R. M. G.; Watkins, D. L. Radically Accessing D-A Type Ambipolar Copolymeric Materials with Intrinsic Electrical Conductivity and Visible-Near Infrared Absorption Via Electro-Copolymerization. Macromol. Chem. Phys. 2019, 220, 1900289.
- (35) Culebras, M.; Gómez, C. M.; Cantarero, A. Enhanced Thermoelectric Performance of PEDOT with Different Counter-Ions Optimized by Chemical Reduction. J. Mater. Chem. A 2014, 2, 10109-10115.
- (36) Zotti, G.; Zecchin, S.; Schiavon, G.; Louwet, F.; Groenendaal, L.; Crispin, X.; Osikowicz, W.; Salaneck, W.; Fahlman, M. Crispin, X, Electrochemical and XPS Studies toward the Role of Monomeric and Polymeric Sulfonate Counterions in the Synthesis, Composition, and Properties of Poly(3,4-Ethylenedioxythiophene). Macromolecules 2003, 36, 470-3344.
- (37) Eftekhari, A.; Jafarkhani, P. Polymerization of Aniline through Simultaneous Chemical and Electrochemical Routes. Polym. J. 2006, 38, 651-658.
- (38) Lv, X.; Li, J.; Xu, L.; Zhu, X.; Tameev, A.; Nekrasov, A.; Kim, G.; Xu, H.; Zhang, C. Colorless to Multicolored, Fast Switching, and Highly Stable Electrochromic Devices Based on Thermally Cross-Linking Copolymer. ACS Appl. Mater. Interfaces 2021, 13, 41826-
- (39) Curiac, C.; Hunt, L. A.; Sabuj, M. A.; Li, Q.; Baumann, A.; Cheema, H.; Zhang, Y.; Rai, N.; Hammer, N. I.; Delcamp, J. H. Probing Interfacial Halogen-Bonding Effects with Halogenated Organic Dyes and a Lewis Base-Decorated Transition Metal-Based Redox Shuttle at a Metal Oxide Interface in Dye-Sensitized Solar Cells. J. Phys. Chem. C 2021, 125, 17647-17659.
- (40) Cheema, H.; Watson, J.; Delcamp, J. Photon management strategies in SSM-DSCs: Realization of a >11% PCE device with a 2.3 V output. Sol. Energy 2020, 208, 747-752.
- (41) Zhang, S.; Li, Y.; Zhang, T.; Cao, S.; Yao, Q.; Lin, H.; Ye, H.; Fisher, A.; Lee, J. Y. Dual-Band Electrochromic Devices with a Transparent Conductive Capacitive Charge-Balancing Anode. ACS Appl. Mater. Interfaces 2019, 11, 48062-48070.
- (42) Sun, H.; Zhang, L.; Dong, L.; Zhu, X.; Ming, S.; Zhang, Y.; Xing, H.; Duan, X.; Xu, J. Aqueous Electrosynthesis of an Electrochromic Material Based Water-Soluble EDOT-MeNH2 Hydrochloride. Synth. Met. 2016, 211, 147-154.

# **□** Recommended by ACS

Design of Dithienopyran-Based Conjugated Polymers for **High-Performance Electrochromic Devices** 

Jinseck Kim, Hong Chul Moon, et al.

IANIIARY 12 2023

CHEMISTRY OF MATERIALS

READ 2

**Electron-Transporting Conjugated Polymers from Novel Aromatic Five-Membered Diimides: Naphtho**[1,2-b:4,3-b']dithiophene and -Diselenophene Diimides

Lingli Zhao, Huajie Chen, et al.

APRIL 05, 2023

MACROMOLECULES

READ **C** 

Alkynyl BODIPY-Core Bridged Perylene Diimide Star-**Shaped Nonfullerene Acceptors for Efficient Polymer Solar** Cells

Xuanlai Zong, Ganesh D. Sharma, et al.

DECEMBER 02 2022

ACS APPLIED ENERGY MATERIALS

RFAD 17

Incorporation of the Benzobisthiadiazole Unit Leads to Open-Shell Conjugated Polymers with n-Type Charge **Transport Properties** 

Xuyang Wei, Gui Yu, et al.

APRIL 07, 2023

MACROMOLECULES

RFAD 🗹

Get More Suggestions >